

Ground State Er^{3+} Ion in the $\text{YGa}_3(\text{BO}_3)_4$

A.A. PROKHOROV^a, L.F. CHERNUSH^b, R. MINIKAYEV^c,
J. LANČOK^a AND A.D. PROKHOROV^{b,*}

^a*Institute of Physics AS CR, Na Slovance 2, 18221 Prague, Czech Republic*

^b*A.A. Galkin Donetsk Institute for Physics and Engineering, R. Luxembourg 72, 83114 Donetsk*

^c*Institute of Physics, Polish Academy of Sciences,
Aleja Lotników 32/46, PL-02668, Warsaw, Poland*

Received: 01.04.2020 & Accepted: 25.08.2020

Doi: [10.12693/APhysPolA.138.777](https://doi.org/10.12693/APhysPolA.138.777)

*e-mail: prokhorov@fzu.cz

The paper presents the results of a ground state study of $\text{YGa}_3(\text{BO}_3)_4$ crystals doped with erbium ions. The EPR spectrum of the Er^{3+} ion, which replaces yttrium ions in a crystal and is located in a slightly distorted prism of six oxygen ions, is detected and decoded. The parameters of the spin Hamiltonian describing the strongly anisotropic behavior of the spectrum are determined $g_{\parallel} = 1.269(1)$, $g_{\perp} = 9.34(6)$, $A_{\parallel} = 47.7(5)$ MHz, $A_{\perp} = 320(9)$ MHz.

topics: EPR, multiferroics, rare-earth, aluminum borates, gallium borates, spin Hamiltonian parameters

1. Introduction

Modern scientific and applied materials science requires both an appearance of new materials with a desired combination of functional properties and an improvement and optimization of physical parameters and structural quality of the already known materials. They are acknowledged for good luminescent and non-linear optical properties like high thermal, chemical and mechanical stability. Weakly-interacting doping ions of rare-earth elements facilitate the abilities of borates to be the bases of compact lasers. An interest in small-size lasers pumped by light emitting diodes of green-blue spectrum stimulates research on new solid-state laser systems based on non-linear crystals [1–3]. Possible doping of the crystals by both rare-earth ions and the ions of the iron group makes them attractive objects from the viewpoint of magnetism because the interaction of two magnetic subsystems results in a number of specific features of magnetic properties. For instance, the interaction between the iron ions in quasi-one-dimensional chains of $\text{GdFe}_3(\text{BO}_3)_4$ results in antiferromagnetic ordering a 37 K and the interaction with the rare-earth subsystem is responsible for a spin-reorientation transition at 10 K [4, 5]. A number of papers have been devoted to studies of EPR spectra in aluminum borates [6–24]. Much less attention was paid to the crystals with $\text{M}=\text{Ga}$ ($\text{ReGa}_3(\text{BO}_3)_4$) that can demonstrate no less interesting properties [25, 26]. The crystals of $\text{RGa}_3(\text{BO}_3)_4$ and the thoroughly studied aluminum borates are reported [27, 28] as belonging

to the same space group R32. The present paper is aimed at a complex study of the magnetic properties of the ground state of the Er^{3+} ions incorporated into the $\text{YGa}_3(\text{BO}_3)_4$ crystals as doping, which includes the study of the EPR.

2. Samples and experimental procedure

The crystals of the borate family $\text{RM}_3(\text{BO}_3)_4$, where R is a rare-earth metal or yttrium and M are trivalent ions of Al, Ga, Fe, Sc, Cr, are crystallized within the huntite structure $\text{CaMg}_3(\text{BO}_3)_4$, the space group R32. Figure 1 shows the crystal structure Er^{3+} -doped $\text{YGa}_3(\text{BO}_3)_4$. A unit cell of gallium borate contains $Z=3$ formula units. Coordination polyhedrons of Y^{3+} , Al^{3+} and B^{3+} are trigonal prisms, octahedrons and triangles formed by oxygen atoms, respectively. Rare-earth ions are located at rotary axes C_3 in slightly distorted prisms with the upper triangles turned around the bottom ones. The ions of Ga^{3+} are positioned in oxygen octahedrons which are linked at the edges to form twisted columns aligned with C_3 -axis. Atoms B_1 and B_2 are located in oxygen triangles of two types: B_1 are placed in the triangles perpendicular to the triple axes and alternating with the Y-prisms and B_2 are located in the triangles connecting the twisted columns of Ga-octahedrons. The crystals of $\text{YGa}_3(\text{BO}_3)_4$ doped by 0.2% Er^{3+} were produced by a spontaneous solution-melt crystallization. $\text{Bi}_2\text{O}_3 + \text{B}_2\text{O}_3$ was used as a solvating agent. The growth was due to cooling of the solution from 900 °C to 700 °C at the rate of 2°/h. The obtained results were transparent faceted crystals of 0.5–1 mm in size.

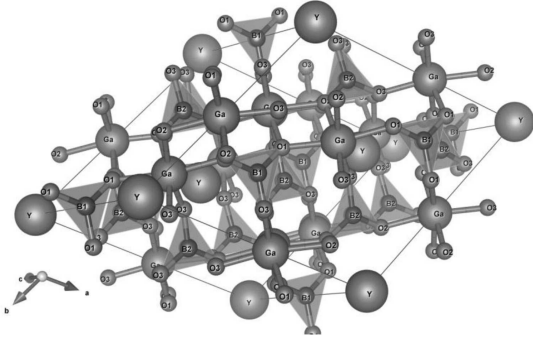


Fig. 1. Crystal structure of $\text{YGa}_3(\text{BO}_3)_4$ doped with Er^{3+} iontylx.

The EPR spectra were measured using X- and Q-band radiation, within the temperature range of 5–300 K. The continuous wave EPR spectra were measured using a Bruker X-/Q-band E580 FT/CW ELEXSYS spectrometer. For the measurements, the ER 4122 SHQE Super X High-Q cavity with the TE011 mode was used. The samples were placed into quartz rods of 4 mm in diameter. The experimental parameters were: microwave frequency — 9.87 GHz, microwave power — 1500 mW, modulation frequency — 100 kHz, modulation amplitude — 0.2 mT and the conversion time — 60 ms.

3. Results and discussion

The Er (0.2%) doped $\text{YGa}_3(\text{BO}_3)_4$ crystal structure was confirmed by X-ray powder diffraction measurements. The values of determined lattice parameters a and c were 9.4520(1) Å and 7.4513(1) Å, respectively. The atomic positions (x, y, z) given for Y/Er(0,0,0), Ga(0.5513(1),0,0), B₁(0,0,0.5), B₂(0.443(1),0,0.5), O₁(0.864(1),0,0.5), O₂(0.588(1),0,0.5), O₃(0.452(1),0.144(1),0.507(1)) were refined by the Rietveld method. These values are in good agreement with the previously [26] reported data for Ga-based borate.

A trivalent ion of Er^{3+} which isovalently replaces in a crystal lattice a gallium borate Y^{3+} ion with the symmetry of D_3 node is characterized by the $4f^{11}$ electron configuration, with the lowest multiplet $^4I_{15/2}$. As f -shell contains an odd number of electrons, in the crystal field of $\text{YGa}_3(\text{BO}_3)_4$, a multiplet is split into eight Kramers doublets with the EPR signal registered at the lowest one. In Fig. 2, the spectrum of Er^{3+} is demonstrated in the case of the magnetic field perpendicular to the C_3 axis.

The spectrum is composed of the central intensive absorption line associated with the even erbium isotopes and eight lines of superfine structure which emerged due to the interaction of the electron spin and the magnetic moment of the nucleus of odd isotope ^{167}Er (the spin is 7/2, the natural occurrence is 22.82%). The spectrum is strongly

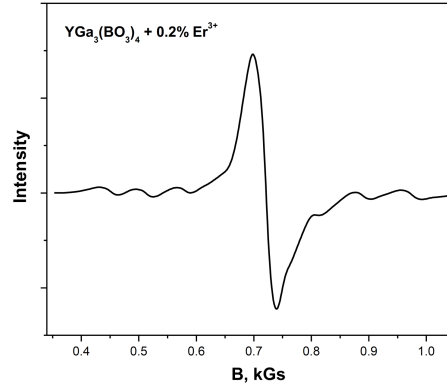


Fig. 2. EPR spectrum of the Er^{3+} ion in $\text{YGa}_3(\text{BO}_3)_4$, $\mathbf{B} \perp C_3$.

anisotropic. The behavior in the magnetic field can be described by a spin Hamiltonian with the effective spin $S = 1/2$ [29]

$$H = g\mu_B \mathbf{S}\mathbf{B} + \mathbf{A}\mathbf{S}\mathbf{I}, \quad (1)$$

where μ_B is the Bohr magneton, \mathbf{B} is the vector of magnetic induction, g is the tensor of the factor of spectroscopic splitting, \mathbf{S} is the operator of the electron spin, \mathbf{I} is the operator of the nuclear spin, \mathbf{A} is the tensor of superfine interaction. Erbium nuclei are characterized by a small quadruple moment besides the magnetic dipole moment. Within the accuracy of the experiment, the quadruple moment was not registered, so the associated terms are not included in the spin Hamiltonian.

The observed Hamiltonian parameters for Er^{3+} ion in the $\text{YGa}_3(\text{BO}_3)_4$ crystal system are $g_{\parallel} = 1.269(1)$, $g_{\perp} = 9.34(6)$, $A_{\parallel} = 47.7(5)$ MHz, $A_{\perp} = 320(9)$ MHz, $g_{\parallel} \times A_{\perp}/g_{\perp} \times A_{\parallel} = 0.913$.

Figure 3 shows the angular dependence of the g -factor. Points determine experimental values, the solid line is the result of the fitting with $g^2 = g_{\parallel}^2 \cos^2(\theta) + g_{\perp}^2 \sin^2(\theta)$, where θ is the angle between the C_3 axis and the direction of the magnetic field. As follows from theory [30], the effect of the crystal field on the basic state of the Er^{3+} ion Er^{3+} (multiplet $^4I_{15/2}$), without taking into account the excited multiplet, gives the ratio $g_{\parallel} \times A_{\perp}/g_{\perp} \times A_{\parallel} = 1$. The obtained experimental value in our case is close to unity, indicating the vanishing effect of higher multiplets of the Er^{3+} ions. Actually, as reported in [31], the neighbor excited multiplet $^4I_{13/2}$ differs from the ground one by 6600 cm^{-1} .

Spin lattice relaxation can be achieved using three main mechanisms. The first mechanism is a direct process in which the spin system and the phonon system exchange a single quantum of energy, that is, a transition takes place from the excited state to the main state accompanied by background radiation equal to the energy distance between the levels. The second mechanism is a combination process, as a result of which the magnetic ion makes a transition from the excited state

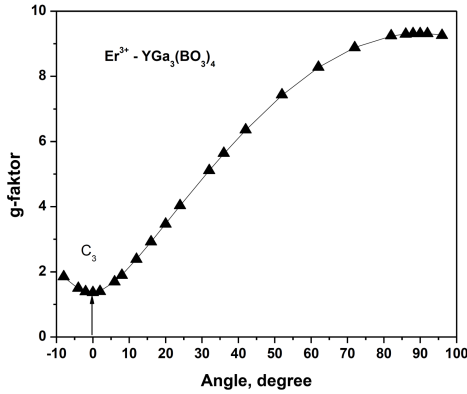


Fig. 3. Dependence of Er^{3+} g -factor in $\text{YGa}_3(\text{BO}_3)_4$ on angle between the C_3 axis and the direction of the magnetic field.

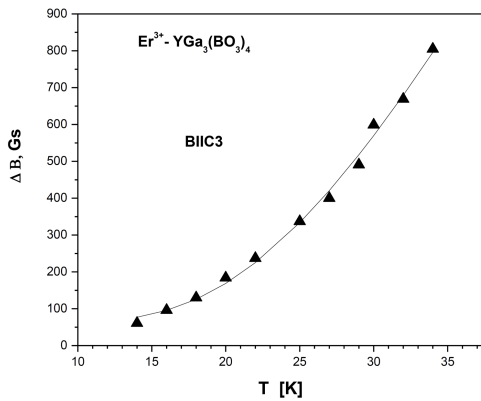


Fig. 4. Dependence of the Er^{3+} ion line width in $\text{YGa}_3(\text{BO}_3)_4$ on temperature in the orientation of $B \parallel C_3$.

to the main state by absorbing one phonon ν_1 and emitting a phonon with frequency ν_2 on the condition that the difference between these frequencies $\nu_2 - \nu_1 = \nu$ is equal to the transition frequency between the states of the paramagnetic ion. The third mechanism is a process of resonance fluorescence (or the Orbach-Aminov process) which takes place with the participation of a real excited state having energy within the phonon on spectrum below the Debye temperature. These three mechanisms participate in spin lattice relaxation but their efficacy may vary significantly.

Temperature dependence of the linewidth presents an opportunity to find the time of spin-lattice relaxation and the relaxation mechanism. The linewidth was determined by the distance between the extreme values of the derivative of the absorption line. Figure 4 shows the dependence of the line width on temperature in orientation when the magnetic field is directed along the C_3 axis. In fact, it is well approximated by the exponential curve characteristic of the Orbach-Aminov process $\Delta B = a + b \exp(-c/k_B T)$, for $a = 68.2$ Gs, $b = 11.6 \times 10^3$ Gs, and $c = 65 \text{ cm}^{-1}$, where T (K) is the temperature and k_B is the Boltzmann constant.

The exponent corresponds to the nearest excited level in the spectrum of Er^{3+} ion in $\text{YGa}_3(\text{BO}_3)_4$ crystal which is 65 cm^{-1} . Due to optical measurements of the Er^{3+} ion spectrum in the isomorphic $\text{YAl}_3(\text{BO}_3)_4$ crystal, the closest excited state has an energy of 47 cm^{-1} [19, 32, 33].

In addition to widening of the EPR line, the shift of the line towards higher field is registered at an increase in temperature and the g -factors are reduced. The magnetic moment of the ground state is modified by the addition of the excited states by the joint action of the Zeeman interaction and the spin-lattice one. The temperature dependence of the shift of the EPR line is proportional to $T^4 \int_0^{\theta/T} dx \frac{x^3}{\exp(x)-1}$ in the Debye model [34, 35]. As the Debye temperature of the tested crystal is 332 K [25], the multiplier of C^4 stays the same in the tested temperature range. On the other hand, the g -factor can be represented as $g(T) = g(0) - \Delta g$, where $\Delta g_{\parallel} = 2.4 \times 10^{-8} T^4$, $\Delta g_{\perp} = 4.2 \times 10^{-7} T^4$. When calculating the temperature shift of the EPR line, it is necessary to take the excited states of the rare-earth ion into account. A lower energy distance to the excited levels makes a higher temperature contribution. The neighbor excited states of the considered ion are rather close.

4. Conclusion

The present paper reports the results of an experimental study of static and dynamic characteristics of the Er^{3+} ions in the crystals of $\text{YGa}_3(\text{BO}_3)_4$. The g -factors and the constants of superfine interaction are found. The ratio $\frac{g_{\parallel} \times A_{\perp}}{g_{\perp} \times A_{\parallel}} = 0.913$ is close to unity which is the evidence of very insignificant admixing of the excited multiplets. A widening of the absorption lines related to temperature increase is associated with a strong spin-phonon interaction in both crystals. Spin-lattice relaxation is well interpreted by means of the Orbach-Aminov processes. A reduction of the g -factor was observed at the temperature rise that was determined by the spin-phonon interaction proportional to T^4 .

Acknowledgments

We acknowledge the Operational Programme Research, Development and Education financed by the European Structural and Investment Funds and the Czech Ministry of Education, Youth and Sports (Project No. SAFMAT-CZ.02.1.01/0.0/0.0/16_013/0001406). The research infrastructure SAFMAT was supported by projects LM2015088 and LO1409 by MEYS.

References

- [1] X.Y. Chen, Z.D. Luo, D. Jaque, J.J. Romero, J.G. Sole, Y.D. Huang, A.D. Jiang, C.Y. Tu, *J. Phys. Condens. Mater.* **13**, 1171 (2001).

- [2] D. Jaque, O. Enguita, J.G. Sole, A.D. Jiang, Z.D. Luo, *Appl. Phys. Lett.* **76**, 2176 (2000).
- [3] A. Brenier, C.Y. Tu, Z.J. Zhu, J.F. Li, Y. Wang, Z.Y. You, B.C. Wu, *Appl. Phys. Lett.* **84**, 16 (2004).
- [4] A.D. Balaev, L.N. Bezmaternykh, I.A. Gudim, V.L. Temerov, S.G. Ovchinnikov, S.A. Kharlamova, *J. Magn. Magn. Mater.* **258–259**, 532 (2003).
- [5] S.A. Kharlamova, S.G. Ovchinnikov, A.D. Balaev, M.F. Thomas, I.S. Lyubutin, A.G. Gavriiliuk, *J. Exp. Theor. Phys.* **101**, 1098 (2005).
- [6] A.A. Prokhorov, A.D. Prokhorov, L.F. Chernush, V.P. Dyakonov, H. Szymczak, A. Dejneka, *Phys. Scr.* **90**, 065804 (2015).
- [7] A.M. Vorotynov, G.A. Petrakovskii, Y.G. Shiyan, L.N. Bezmaternykh, V.E. Temerov, A.F. Bovina, P. Aleshkevych, *Phys. Solid State* **49**, 463 (2007).
- [8] C. Rudowicz, P. Gnutek, M. Acikgoz, *Opt. Mater.* **46**, 254 (2015).
- [9] M. Acikgoz, P. Gnutek, C. Rudowicz, *Opt. Mater.* **36**, 1342 (2014).
- [10] A.A. Prokhorov, L.P. Chernush, V. Babin, M. Buryi, D. Savchenko, J. Lancok, M. Nikl, A.D. Prokhorov, *Opt. Mater.* **66**, 428 (2017).
- [11] A.A. Prokhorov, L.F. Chernush, V.P. Dyakonov, H. Szymczak, A.D. Prokhorov, *J. Magn. Magn. Matter* **420**, 285 (2016).
- [12] J.P.R. Wells, M. Yamaga, T.P.J. Han, M. Honda, *J. Phys. Condens. Matter* **15**, 539 (2003).
- [13] A.D. Prokhorov, E.E. Zubov, A.A. Prokhorov, L.F. Chernush, R. Minyakaev, V.P. Dyakonov, H. Szymczak, *Phys. Status Solidi B* **250**, 1331 (2013).
- [14] A.A. Prokhorov, *J. Mater. Sci.* **51**, 4762 (2016).
- [15] M. Acikgoz, C. Rudowicz, P. Gnutek, *Opt. Mater.* **73**, 124 (2017).
- [16] V.A. Atsarkin, V.B. Kravchen, I.G. Matveeva, *Sov. Phys. Solid State.* **9**, 2646 (1968).
- [17] G. Wang, H.G. Gallagher, T.P.J. Han, B. Henderson, M. Yamaga, T. Yosida, *J. Phys. Condens. Matter* **9**, 1649 (1997).
- [18] A. Watterich, P. Aleshkevych, M.T. Borowiec, T. Zayarnyuk, H. Szymczak, E. Beregi, L. Kovacs, *J. Phys. Condens. Matter* **15**, 3323 (2003).
- [19] A.D. Prokhorov, A.A. Prokhorov, L.F. Chernysh, P. Aleshkevich, V. Dyakonov, H. Szymczak, *J. Magn. Magn. Mater.* **326**, 162 (2013).
- [20] A.D. Prokhorov, I.N. Krygin, A.A. Prokhorov, L.F. Chernush, P. Aleshkevich, V. Dyakonov, H. Szymczak, *Phys. Status Solidi A* **206**, 2617 (2009).
- [21] A.D. Prokhorov, A.A. Prokhorov, L.F. Chernysh, V.P. Dyakonov, H. Szymczak, *J. Magn. Magn. Mater.* **323**, 1546 (2011).
- [22] A.D. Prokhorov, A.A. Prokhorov, E.E. Zubov, L.F. Chernysh, V. Dyakonov, H. Szymczak, *Low Temp. Phys.* **40**, 730 (2014).
- [23] A.D. Prokhorov, A.A. Prokhorov, L.F. Chernush, R. Minyakaev, V.P. Dyakonov, H. Szymczak, *Phys. Status Solidi B* **251**, 201 (2014).
- [24] A.D. Prokhorov, M.T. Borowiec, M.C. Pujol, I.M. Krygin, A.A. Prokhorov, V.P. Dyakonov, P. Aleshkevych, T. Zayarnyuk, H. Szymczak, *Eur. Phys. J. B* **55**, 389 (2007).
- [25] A.A. Prokhorov, L.F. Chernush, R. Minyakaev, A. Mazur, T. Zajarniuk, A. Szewczyk, V. Dyakonov, J. Lancok, A.D. Prokhorov, *J. Alloy Compd.* **765**, 710 (2018).
- [26] A.A. Prokhorov, L.F. Chernush, T.N. Melnik, R. Minikayev, A. Mazur, V. Babin, M. Nikl, J. Lancok, A.D. Prokhorov, *Sci. Rep.* **9**, 12787 (2019).
- [27] N.I. Leonyuk, L.I. Leonyuk, *Prog. Cryst. Growth Charact.* **31**, 179 (1995).
- [28] L.I. Alshinskaya, N.I. Leonyuk, T.I. Timchenko, *Krist. Tech.* **14**, 897 (1979).
- [29] S.A.A.B.M. Kozyrev, *Electron Paramagnetic Resonance*, Izd. Nauka, Moskva 1972, p. 362.
- [30] A. Abragam, B. Bleaney, *Electron Paramagnetic Resonance of Transition Ions*, OUP Oxford, 2012 P. 928.
- [31] M. Dammak, *J. Alloys Compd.* **393**, 51 (2005).
- [32] M. Mazzerà, A. Baraldi, R. Capelletti, E. Beregi, I. Foldavir, *Phys Status Solidi C* **4**, 860 (2007).
- [33] A. Baraldi, R. Capelletti, N. Magnani, M. Mazzerà, E. Beregi, I. Foldvari, *J. Phys. Condens. Matter* **17**, 6245 (2005).
- [34] C.A. Bates, H. Szymczak, *Phys. Status Solidi B* **74**, 225 (1976).
- [35] C.A. Bates, H. Szymczak, *Z. Phys. B Condes. Matter* **28**, 67 (1977).